Proton charge radius and its consistency with the experiments

C. Adamuščín, **E. Bartoš**, S. Dubnička, A.-Z. Dubničková

Institute of Physics SAS, Bratislava, Slovakia
Dept. of Theoretical Physiscs, Comenius University, Bratislava, Slovakia

6. October 2016

2–8 October 2016
Budva, Becici, Montenegro

Outlook

Abstract

In presented work the new result for the value of proton charge root mean square radius in the framework of Unitary and Analytic model of proton electromagnetic structure is announced. The obtained result is compatible with the value obtained by spectroscopy of the muon hydrogen target based on precision measurement of the Lamb shift. The analysis of experimental information on the data from unpolarized elastic scattering and polarization transfer processes is given in the second part of the talk.

Motivation

1. **ep elastic scattering** world data experiments $\rightarrow$ rms charge radius value
2. **muonic hydrogen** laser spectroscopy precise measurements

$$\Downarrow$$

"proton radius puzzle"

discrepancy between the measured Lamb shift in muonic hydrogen and its expected value

CREMA Collaboration – HyperMu

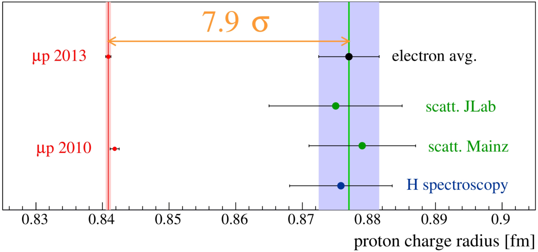

Paul Scherrer Institute PSI (CH) – Lambshift in Muonic Hydrogen

"Proton structure from the measurement of 2S-2P transition frequencies of muonic hydrogen", Antognini et al., **Science 339, 417-420 (2013)**

"The size of the proton", R. Pohl et al., **Nature, vol. 466, issue 7303, pp. 213-216 (2010)**

Hydrogen energy levels

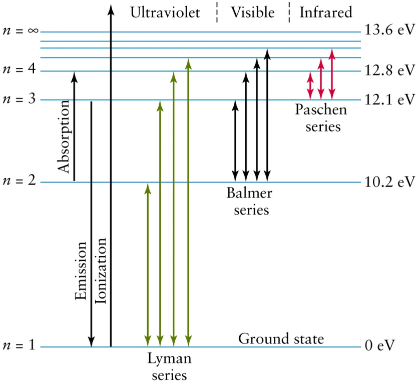

Rydberg formula for H

$$\frac{1}{\lambda} = R_\infty \left(\frac{1}{n_1^2} - \frac{1}{n_2^2} \right), \quad R_\infty = \frac{m_e e^4}{8 \varepsilon_0^2 h^3 c}$$

Rydberg constant

$$R_\infty = 1.0973731568508(65) \times 10^7 \,\mathrm{m}^{-1}$$
$$1\mathrm{Ry} \equiv hcR_\infty = 13.605693009(84)\,\mathrm{eV}$$

high precision

Hydrogen spectroscopy

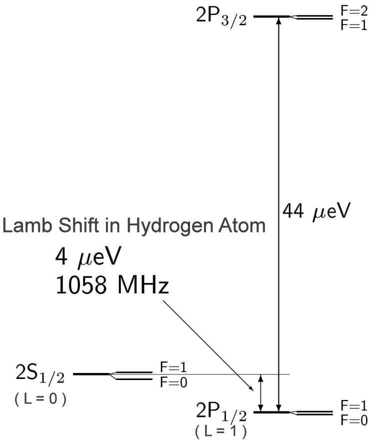

Hydrogen energy for S-state levels (sensitivity to **Lamb shift**)

$$E(nS) = \frac{R}{n^2} + \frac{L_{1S}}{n^3}$$

$$R = R_\infty c =$$

$$= 3.289841960355(19) \times 10^{15}\,\mathrm{Hz}$$

$$L_{1S} \simeq 8171.636(4)\,[\mathrm{MHz}] + 1.5645\,[\mathrm{MHz/fm^2}]\mathbf{r_p^2}$$

p charge radius from atomic hydrogen

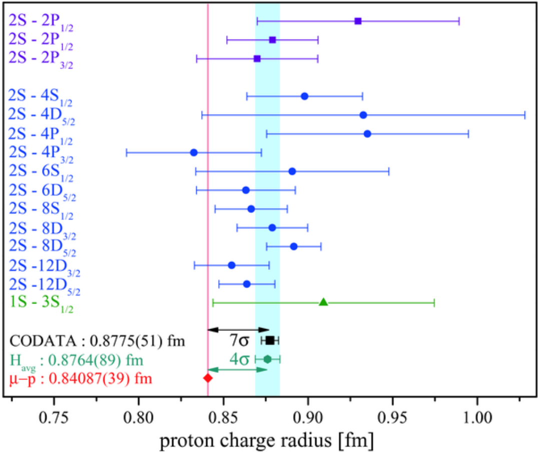

Results from radio frequency measurements of the 2S-2P Lamb shift (violet) and optical transition frequencies (blue). The discrepancy between hydrogen and muonic hydrogen value [Beyer et al., 2013].

Muonic hydrogen

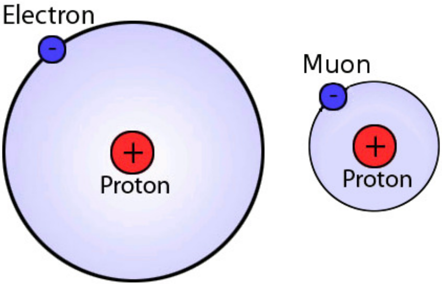

$$m_\mu = 105.6583715\,\mathrm{MeV} \sim 200 m_e$$

$\sim 200\times$ smaller Bohr orbits

$\sim 200^3\times$ larger overlap of wave functions

we know R, from Lamb shift we want **find r_p radius**

Energy levels in muonic hydrogen for $n = 2$

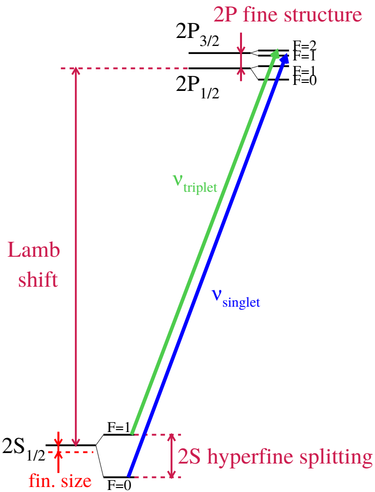

Lamb shift

splitting $2S_{1/2}$ — $2P_{1/2}$

$\sim \alpha^3 R$

$\sim r_p$ radius

r_p contribution to LS $\sim 1.8\%$

Hyperfine splitting

$\sim$ Zemach radius

Z. radius contribution to HS $\sim 0.8\%$

[Antognini et al., 2013a]

Muonic hydrogen – [Antognini et al., 2016]

measured transition $\begin{cases} \text{triplet states:} & 2S_{1/2}^{F=1} - 2P_{3/2}^{F=2} \\ \text{singlet states:} & 2S_{1/2}^{F=0} - 2P_{3/2}^{F=1} \end{cases}$

$$\Delta E_L = \frac{1}{4} h\nu_s + \frac{3}{4} h\nu_t - 8.8123(3)\,\mathrm{meV}$$

$$\Delta E_{HFS} = h\nu_s - h\nu_t + 3.2480(2)\,\mathrm{meV}$$

$\Delta E_L^{exp} = 202.3706(23)\,\mathrm{meV}$ for frequency $48932.99(55)\,\mathrm{GHz}$

$$\Delta E_L^{th} = \underbrace{206.0336(15)\,[\mathrm{meV}]}_{QED} - \underbrace{5.2275(10)\,[\mathrm{meV/fm}^2] r_p^2}_{size\ effects} + \underbrace{0.0332(20)\,[\mathrm{meV}]}_{TPE}$$

muon experiment

$r_p = 0.84087(39)\,\mathrm{fm}$

CODATA ep

$r_p = 0.8775(51)\,\mathrm{fm}$

Muonic hydrogen – [Antognini et al., 2016]

measured transition $\begin{cases} \text{triplet states:} & 2S_{1/2}^{F=1} - 2P_{3/2}^{F=2} \\ \text{singlet states:} & 2S_{1/2}^{F=0} - 2P_{3/2}^{F=1} \end{cases}$

$$\Delta E_L = \frac{1}{4}h\nu_s + \frac{3}{4}h\nu_t - 8.8123(3)\,\mathrm{meV}$$
$$\Delta E_{HFS} = h\nu_s - h\nu_t + 3.2480(2)\,\mathrm{meV}$$

$$\Delta E_L^{exp} = 202.3706(23)\,\mathrm{meV} \qquad \text{for frequency} \quad 48932.99(55)\,\mathrm{GHz}$$

$$\Delta E_L^{th} = \underbrace{206.0336(15)\,[\mathrm{meV}]}_{QED} - \underbrace{5.2275(10)\,[\mathrm{meV/fm^2}]r_\mathrm{p}^2}_{size\ \ effects} + \underbrace{0.0332(20)\,[\mathrm{meV}]}_{TPE}$$

muon experiment

$$r_\mathrm{p} = 0.84087(39)\,\mathrm{fm}$$

CODATA ep

$$r_\mathrm{p} = 0.8775(51)\,\mathrm{fm}$$

Note on Zemach moment

[Pohl et al., 2010, Antognini et al., 2013b]

$$\Delta E_L^{th} = 209.9779(49)\,[\mathrm{meV}] - 5.2262\,[\mathrm{meV/fm}^2] r_\mathrm{p}^2 + 0.00913\,[\mathrm{meV}] \langle\, r_\mathrm{p}^3 \,\rangle_{(2)}$$

updated results [Antognini et al., 2013a]

$$\Delta E_L^{th} = 206.0336(15)\,[\mathrm{meV}] - 5.2275(10)\,[\mathrm{meV/fm}^2] r_\mathrm{p}^2 + 0.0332(20)\,[\mathrm{meV}]$$

$$\Delta E_{HFS}^{th} = 22.9763(15)\,[\mathrm{meV}] - 0.1621(10)\,[\mathrm{meV/fm}^2] r_Z + 0.0080(26)\,[\mathrm{meV}]$$

third Zemach moment & proton charge distribution:

$$\langle\, r_\mathrm{p}^3 \,\rangle_{(2)} \equiv \int \mathrm{d}^3 r\, r^3 \rho_{(2)}(r), \quad \rho_{(2)}(r) = \int \mathrm{d}^3 r' \rho_\mathrm{p}(|\vec{r} - \vec{r}'|)\rho_\mathrm{p}(\vec{r}')$$

$$\langle\, r_\mathrm{p}^3 \,\rangle_{(2)} = 2.71(13)\,\mathrm{fm}^3 \text{ and } 2.85(8)\,\mathrm{fm}^3$$

p charge radius from atomic hydrogen

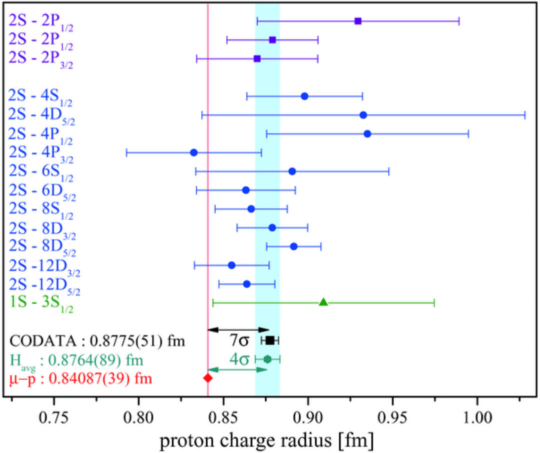

Results from radio frequency measurements of the 2S-2P Lamb shift (violet) and optical transition frequencies (blue). The discrepancy between hydrogen and muonic hydrogen value [Beyer et al., 2013].

Proton charge radius $\langle r_p^2 \rangle$

upper bound on Z. moment: $\langle r_p^3 \rangle_{(2)} = \frac{48}{\pi} \int_0^\infty \frac{dq}{q^4} \left[G_E^p(q^2)^2 + \frac{q^2}{3} \langle r_p^2 \rangle - 1 \right]$

p charge density: $\rho_p(r) \equiv \int \frac{d^3 q}{(2\pi)^3} e^{-i\vec{q}\vec{r}} G_E^p(\vec{q}^2)$

p charge radius: $\langle r_p^2 \rangle \equiv \int d^3 r r^3 \rho_p(r), \qquad t = q^2 = -Q^2$

$\Longrightarrow \langle r_p^2 \rangle = \int_0^\infty r^2 \rho_p(r) 4\pi r^2 dr$ or $\langle \mathbf{r_p^2} \rangle = -6 \frac{d G_E^p(Q^2)}{d Q^2} \Big|_{Q^2 \to 0}$

- precise extraction of $\langle \mathbf{r_p^2} \rangle$ from electron–proton scattering data
- adequate form factor to analyze low-energy data

Unpolarized scattering $e^- p \to e^- p \Longrightarrow$ cross section determination

$$\left(\frac{d\sigma}{d\Omega}\right)_0 = \left(\frac{d\sigma}{d\Omega}\right)_{\mathrm{Mott}} \left[A(Q^2) + B(Q^2)\tan^2\frac{\theta}{2}\right]$$

$$A(Q^2) = \frac{G_E^{p\,2}(Q^2) + \tau G_M^{p\,2}(Q^2)}{1+\tau}, \quad B(Q^2) = 2\tau G_M^{p\,2}(Q^2)$$

$$\left(\frac{d\sigma}{d\Omega}\right)_0 = \left(\frac{d\sigma}{d\Omega}\right)_{\mathrm{Mott}} \frac{\varepsilon G_E^{p\,2} + \tau G_M^{p\,2}}{\varepsilon(1+\tau)}$$

$$\tau = Q^2/(4m_p^2), \quad \varepsilon = \left[1 + 2(1+\tau)\tan^2\frac{\theta}{2}\right]^{-1}$$

Data for low Q^2 values

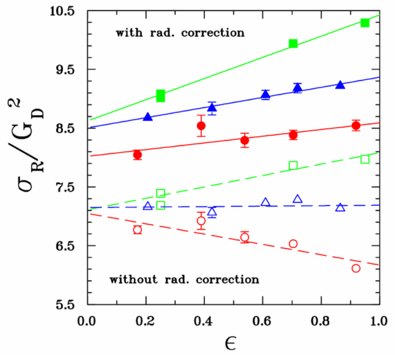

Rosenbluth separation technique

$$\sigma_R = \frac{\left(\frac{\mathrm{d}\sigma}{\mathrm{d}\Omega}\right)_0}{\left(\frac{\mathrm{d}\sigma}{\mathrm{d}\Omega}\right)_{Mott} \frac{\varepsilon(1+\tau)}{\tau}}$$

$$\sigma_R = \varepsilon \underbrace{\frac{1}{\tau} {G_E^p}^2}_{slope} + \underbrace{{G_M^p}^2}_{intercept}$$

attempt with continued-fraction expansion method [Sick]

$r_p = 0.895(18)\,\mathrm{fm}$

Data for low Q^2 values

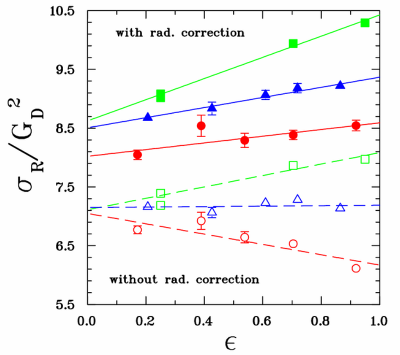

Rosenbluth separation technique

$$\sigma_R = \frac{\left(\frac{d\sigma}{d\Omega}\right)_0}{\left(\frac{d\sigma}{d\Omega}\right)_{Mott} \frac{\varepsilon(1+\tau)}{\tau}}$$

$$\sigma_R = \varepsilon \underbrace{\frac{1}{\tau} G_E^{p\,2}}_{slope} + \underbrace{G_M^{p\,2}}_{intercept}$$

attempt with continued-fraction expansion method [Sick]

$$r_p = 0.895(18)\,\mathrm{fm}$$

Reanalysis

Reanalysis of the Rosenbluth data in terms of the electric to magnetic form factor squared ratio R [Pacetti and Gustafsson, 2016]

$$\sigma_{\rm red} = G_{\rm M}^2 (R^2 \varepsilon + \tau)$$

$$R = G_{\rm E}/G_{\rm M}$$

$\mu^2 R^2$ as a function of Q^2 for Analysis II (red) and Analysis III (blue)

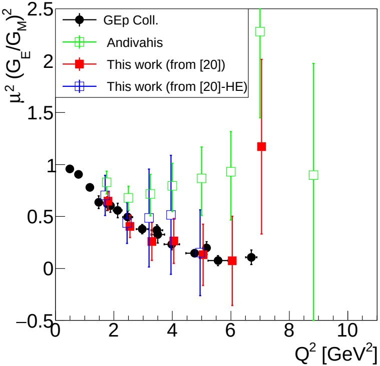

Polarization transfer process
$\vec{e}\,p \to e\,\vec{p} \Longrightarrow$ determination of polarization variables

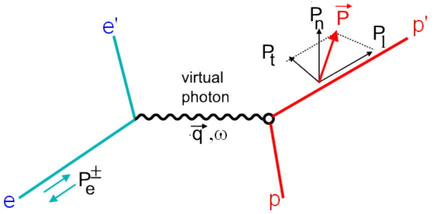

recoil proton $\vec{p}$

$$\begin{cases} P_t = -\frac{2h}{I_0}\sqrt{\tau(1+\tau)}\,G_E^p G_M^p \tan\frac{\theta}{2}, \\ P_\ell = \frac{h}{m_p I_0}\left(E_e + E_{e'}\right)\sqrt{\tau(1+\tau)}\,{G_M^p}^2 \tan^2\frac{\theta}{2} \end{cases}$$

$$\frac{G_E^p}{G_M^p} = -\frac{P_t}{P_\ell}\frac{(E_e + E_{e'})}{2m_p}\tan\frac{\theta}{2}$$

How construct form factors?

- **Unknown exact functional form** of nucleon FFs
- FFs **do not have** dipole/polynomial/spline/. . . functional form
- But: there exists plethora of **models** based on:

dipole $G_{\mathrm{D}} = \left(1 + Q^2/0.71\right)^{-2}$, double dipole, polynomial models, splines, Friedrich-Walcher p., continued fraction, bounded polynomial z-expansion (conformal mapping [Hill and Paz, 2010])

$\rightarrow r_{\mathrm{p}} = 0.879(8)\,\mathrm{fm}$ (even after TPE effects)

(see [Bernauer et al., 2014])

How construct form factors?

- **Unknown exact functional form** of nucleon FFs
- FFs **do not have** dipole/polynomial/spline/... functional form
- But: there exists plethora of **models** based on:

dipole $G_{\mathrm{D}} = \left(1 + Q^2/0.71\right)^{-2}$, double dipole, polynomial models, splines, Friedrich-Walcher p., continued fraction, bounded polynomial z-expansion (conformal mapping [Hill and Paz, 2010])

$\rightarrow r_{\mathrm{p}} = 0.879(8)\,\mathrm{fm}$ (even after TPE effects)

(see [Bernauer et al., 2014])

Nucleon matrix of EM current

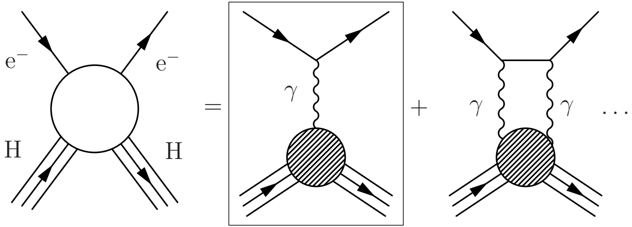

$$\langle \mathrm{N} \,|\, J_\mu^{\mathrm{EM}} \,|\, \mathrm{N} \rangle = e\bar{\mathrm{u}}(p')\Big\{\gamma_\mu F_1(t) + \frac{\mathrm{i}}{2m_{\mathrm{N}}}\sigma_{\mu\nu}(p'-p)_\nu F_2(t)\Big\}\mathrm{u}(p)$$

$$G_{\mathrm{E}}(t) = F_1(t) + \frac{t}{4m_{\mathrm{N}}^2}F_2(t) \qquad G_{\mathrm{M}}(t) = F_1(t) + F_2(t)$$

Nucleons

Sachs FF: $G_{\mathrm{E}}^{\mathsf{p}}$, $G_{\mathrm{M}}^{\mathsf{p}}$, $G_{\mathrm{E}}^{\mathsf{n}}$, $G_{\mathrm{M}}^{\mathsf{n}}$ Dirac and Pauli FF: F_1^{p}, F_1^{n}, F_2^{p}, F_2^{n}

$$G_{\mathrm{E}}^{\mathsf{p}}(t) = G_{\mathrm{E}}^{s}(t) + G_{\mathrm{E}}^{v}(t) = F_1^{\mathsf{p}}(t) + \frac{t}{4m_{\mathsf{N}}^2} F_2^{\mathsf{p}}(t),$$

$$G_{\mathrm{M}}^{\mathsf{p}}(t) = G_{\mathrm{M}}^{s}(t) + G_{\mathrm{M}}^{v}(t) = F_1^{\mathsf{p}}(t) + F_2^{\mathsf{p}}(t),$$

$$G_{\mathrm{E}}^{\mathsf{n}}(t) = G_{\mathrm{E}}^{s}(t) - G_{\mathrm{E}}^{v}(t) = F_1^{\mathsf{n}}(t) + \frac{t}{4m_{\mathsf{N}}^2} F_2^{\mathsf{n}}(t),$$

$$G_{\mathrm{M}}^{\mathsf{n}}(t) = G_{\mathrm{M}}^{s}(t) - G_{\mathrm{M}}^{v}(t) = F_1^{\mathsf{n}}(t) + F_2^{\mathsf{n}}(t)$$

U&A model I

1. The experimental fact of creation of unstable vector meson resonances in the $e^+ e^-$ annihilation processes into hadrons.
2. Analytic properties of nucleon EM FF: a. function in complex t-plane besides the cut from $t = 4m_\pi^2$ up to ∞, branch point of square-root type, resonance poles
3. **reality** and **unitarity** conditions
4. correct **normalizations** at $t = 0$

$$G_E^p(0) = 1, \quad G_M^p(0) = \mu_p$$

$$G_E^n(0) = 0, \quad G_M^n(0) = \mu_n$$

conformal mapping $W(t)$ of Riemann sheets

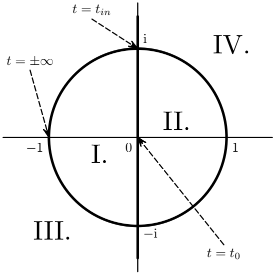

U&A model II

5. Asymptotic behavior of nucleon EM FF followed from the quark model of hadrons: $F(t) \sim t^{1-n_q}$, n_q – constituent quarks.

$$F_{1,2}^{\mathrm{p,n}}(t) = \overbrace{\left(\frac{1-W^2}{1-W_{\mathrm{N}}^2}\right)^{\mathbf{2n}}}^{\text{asymptotic}\sim t^{-n}} \overbrace{\left\{(\dots)\frac{f_{\omega\mathrm{NN}}^{1,2}}{f_\omega} + (\dots)\frac{f_{\phi\mathrm{NN}}^{1,2}}{f_\phi} + (\dots)\frac{f_{\rho\mathrm{NN}}^{1,2}}{f_\rho} + \dots\right\}}^{\text{resonance term}}$$

SU(3) symmetry: ω', ϕ', ρ' ω'', ϕ'', ρ'' complete families

6. all experimental information in SL and TL:
including $\mu_{\mathrm{p}} G_{\mathrm{E}}^{\mathrm{p}}(t)/G_{\mathrm{M}}^{\mathrm{p}}(t)$ and $\mu_{\mathrm{n}} G_{\mathrm{E}}^{\mathrm{n}}(t)/G_{\mathrm{M}}^{\mathrm{n}}(t)$ from polarization exp. $(t < 0)$;
data w/out diff. cross section data of Mainz;
$|G_{\mathrm{E}}^{\mathrm{p}}(t)|$, $|G_{\mathrm{E}}^{\mathrm{n}}(t)|$ for $t > 0$ only from exp. if $|G_{\mathrm{E}}^{\mathrm{p}}(t)| = |G_{\mathrm{M}}^{\mathrm{p}}(t)|$,
$|G_{\mathrm{E}}^{\mathrm{n}}(t)| = |G_{\mathrm{M}}^{\mathrm{n}}(t)|$

Proton form factors

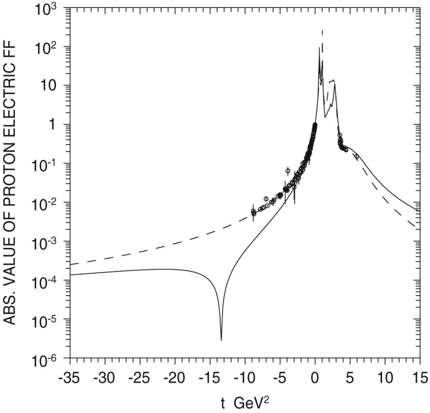

Theoretical behavior of proton electric and magnetic form factors.

Neutron form factors

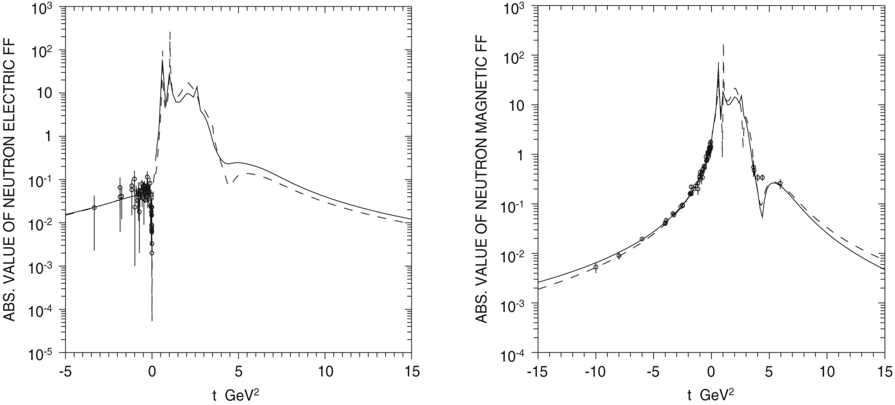

Theoretical behavior of neutron electric and magnetic form factors.

Proton form factors

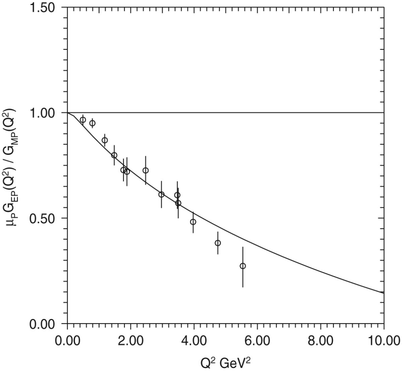

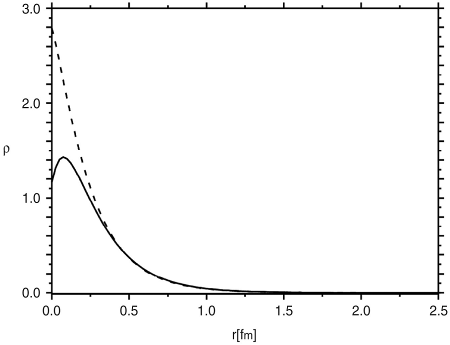

(left) JLab polarization data with U&A fit, (right) charge distribution

Some values of proton rms charge radius

process & source	r_p [fm]
ep scattering MAMI A1 2014	0.879(8)
H spectroscopy avg.	0.8764(89)
continued fraction expansion [Sick]	0.897(18)
[Hill and Paz, 2010]	0.870(26)
dispersion analysis Mainz [U.-M.]	0.84(1)
our result	0.8489(7)
muonic hydrogen 2010	0.8418(7)
muonic hydrogen 2013	0.8409(4)

Expected muon experiments I

- **PRad collaboration (Hall B @ Jefferson Lab):** magnetic-spectrometer-free ep scattering experiment, to use calorimetric method for the first time, extraction of $G_{\mathrm{E}}^{\mathrm{p}}$ at low Q^2 $2 \cdot 10^{-4} - 2 \cdot 10^{-2}\,\mathrm{GeV}^2$ with improved systematic uncertainties
- **A1 collaboration (MAMI @ Mainz):** initial state radiation, determination of $G_{\mathrm{E}}^{\mathrm{p}}$ for Q^2 as low as $10^{-4}\,(\mathrm{GeV/c})^2$)
- **Deuteron scattering (Mainz):** high-precision measurement of elastic $A(Q^2)$ in $\mathrm{d(e,e')d}$ process
- **MUSE collaboration (Paul-Scherrer Institute):** elastic scattering of $\mathrm{e}^{\pm}$, $\mu^{\pm}$ probes on proton in $0.002 - 0.07\,\mathrm{GeV}^2$; study of two-photon-exchange effects due to reverse charge; extraction of p charge radius from ep and μp scattering with high accuracy

Expected muon experiments II

- **NIST, USA**: measurement of Rydberg const. by using Rydberg states (very high-lying states), negligible effect of p size
- **PNPI, Gatchina** proposal to perform in MAMI @ Mainz: high precision measurements of ep differential cross sections at small t-values with the recoiled proton detector (Vorobyev, HSQCD2016)

Hydrogen spectroscopy experiments

Hydrogen energy for S-state levels (sensitivity to Lamb shift)

$$E(nS) = \frac{R}{n^2} + \frac{L_{1S}}{n^3},$$
$$L_{1S} \simeq 8171.636(4)\,[\mathrm{MHz}] + 1.5645\,[\mathrm{MHz/fm}^2]\,r_p^2$$

Improvement of Rydberg constant and proton rms charge radius:

- **Max-Planck-Institute of Quantum Optics @ Garching:** spectroscopy of the 2S-4P transition (A. Beyer et al.) new results?

  (2nd ECT* Workshop on the Proton Radius Puzzle, June 19-25, 2016 Trento, Italy)
- **MPIQO & Laboratoire Kastler Brossel @ Paris:** spectroscopy of the 1S-3S transition
- **York University (Canada):** hydrogen 2S-2P Lamb shift

Conclusions and summary

- We have performed **global analysis** of all existing nucleon EM FF data **by U&A model** of nucleon EM structure.
- Non-dipole behavior of $G_{\mathrm{E}}^{\mathrm{p}}(Q^2)$ with the zero around $Q^2 = 13\,\mathrm{GeV}^2$ has been found.
- We have received $r_{\mathrm{p}} = 0.84894(690)\,\mathrm{fm}$, **compatible** with the value $r_{\mathrm{p}} = 0.84087(39)\,\mathrm{fm}$ obtained in the muon hydrogen atom spectroscopy experiment.
- **Consistency** between ep scattering experiments and laser spectroscopy experiments with muonic hydrogen is preserved.
- We look forward for **new experiments** on both sides.

References I

Antognini, A., Kottmann, F., Biraben, F., Indelicato, P., Nez, F., and Pohl, R. (2013a).
Theory of the 2s–2p lamb shift and 2s hyperfine splitting in muonic hydrogen.
Annals of Physics, 331:127 – 145.

Antognini, A., Nez, F., Schuhmann, K., Amaro, F., Biraben, F., Cardoso, J., Covita, D., Dax, A., Dhawan, S., Diepold, M., Fernandes, L., Giesen, A., Gouvea, A., Graf, T., Hänsch, T., Indelicato, P., Julien, L., Kao, C.-Y., Knowles, P., Kottmann, F., Le Bigot, E.-O., Liu, Y.-W., Lopes, J., Ludhova, L., Monteiro, C., Mulhauser, F., Nebel, T., Rabinowitz, P., Dos Santos, J., Schaller, L., Schwob, C., Taqqu, D., Veloso, J., Vogelsang, J., and Pohl, R. (2013b).

References II

Proton structure from the measurement of 2s-2p transition frequencies of muonic hydrogen.
Science, 339(6118):417–420.

Antognini, A., Schuhmann, K., Amaro, F., Amaro, P., Abdou-Ahmed, M., Biraben, F., Chen, T.-L., Covita, D., Dax, A., Diepold, M., Fernandes, L., Franke, B., Galtier, S., Gouvea, A., Götzfried, J., Graf, T., Hänsch, T., Hildebrandt, M., Indelicato, P., Julien, L., Kirch, K., Knecht, A., Kottmann, F., Krauth, J., Liu, Y.-W., Machado, J., Monteiro, C., Mulhauser, F., Nez, F., Santos, J., Dos Santos, J., Szabo, C., Taqqu, D., Veloso, J., Voss, A., Weichelt, B., and Pohl, R. (2016).
Experiments towards resolving the proton charge radius puzzle.
EPJ Web of Conferences, 113.

References III

Bernauer, J. C., Distler, M. O., Friedrich, J., Walcher, T., Achenbach, P., Ayerbe Gayoso, C., Böhm, R., Bosnar, D., Debenjak, L., Doria, L., Esser, A., Fonvieille, H., Gómez Rodríguez De La Paz, M., Friedrich, J. M., Makek, M., Merkel, H., Middleton, D. G., Müller, U., Nungesser, L., Pochodzalla, J., Potokar, M., Sánchez Majos, S., Schlimme, B. S., Širca, S., and Weinriefer, M. (2014).
Electric and magnetic form factors of the proton.
Physical Review C - Nuclear Physics, 90(1).

Beyer, A., Alnis, J., Khabarova, K., Matveev, A., Parthey, C. G., Yost, D. C., Pohl, R., Udem, T., Hänsch, T. W., and Kolachevsky, N. (2013).
Precision spectroscopy of the 2s-4p transition in atomic hydrogen on a cryogenic beam of optically excited 2s atoms.
Annalen der Physik, 525(8-9):671–679.

References IV

Hill, R. and Paz, G. (2010).
Model-independent extraction of the proton charge radius from electron scattering.
Physical Review D - Particles, Fields, Gravitation and Cosmology, 82(11).
cited By 28.

Pacetti, S. and Gustafsson, E. T. (2016).
Form factor ratio from unpolarized elastic electron proton scattering.

References V

Pohl, R., Antognini, A., Nez, F., Amaro, F., Biraben, F., Cardoso, J., Covita, D., Dax, A., Dhawan, S., Fernandes, L., Giesen, A., Graf, T., Hänsch, T., Indelicato, P., Julien, L., Kao, C.-Y., Knowles, P., Le Bigot, E.-O., Liu, Y.-W., Lopes, J., Ludhova, L., Monteiro, C., Mulhauser, F., Nebel, T., Rabinowitz, P., Dos Santos, J., Schaller, L., Schuhmann, K., Schwob, C., Taqqu, D., Veloso, J., and Kottmann, F. (2010).
The size of the proton.
Nature, 466(7303):213–216.